5022 *Chem. Mater.* **2010,** *22,* 5022–5030
DOI:10.1021/cm101591p

CHEMISTRY OF MATERIALS
Article

Hybrid Supercapacitor Based on Coaxially Coated Manganese Oxide on Vertically Aligned Carbon Nanofiber Arrays

Jianwei Liu,[†] Jeremy Essner, and Jun Li*

Department of Chemistry, Kansas State University, Manhattan, Kansas 66506

Received June 8, 2010. Revised Manuscript Received July 27, 2010

Hybrid supercapacitor electrodes with remarkable specific capacitance have been fabricated by coaxially coating manganese oxide thin films on a vertically aligned carbon nanofiber array. Ultrathin manganese oxide layers are uniformly coated around each carbon nanofiber via cathodic electrochemical deposition, likely based on water electrolysis initiated electrochemical oxidation. This results in a unique core-shell nanostructure which uses the three-dimensional brush-like vertical carbon nanofiber array as the highly conductive and robust core to support a large effective surface area and provide reliable electrical connection to a thin redox active manganese oxide shell. The pseudo-capacitance of 313 F/g in addition to the electrical double layer capacitance of 36 F/g is achieved by cyclic voltammetry at a scan rate of 50 mV/s and maintains at this level as the scan rate is increased up to 2000 mV/s. A maximum specific capacitance of 365 F/g has been achieved with chronopotentiometry in 0.10 M Na_2SO_4 aqueous solution with ~7.5 nm thick manganese oxide. This hybrid core-shell nanostructure demonstrates high performance in maximum specific energy (32.5 Wh/kg), specific power (6.216 kW/kg), and cycle stability (~11% drop after 500 cycles), which are derived from cyclic voltammetry and galvanostatic charge−discharge measurements. This new architecture can be potentially developed as multifunctional electrical energy storage devices.

Introduction

High-performance electrical energy storage (EES) technologies are critical for applications from portable electronics to hybrid electric vehicles. Particularly, efficient storage and release of electrical energy may enable uninterrupted utilization of electricity generated from intermittent renewable energy sources.[1,2] In general, there are two main EES devices, that is, batteries that store and release energy in chemical form through Faradaic redox reactions, and capacitors that store and release electrical energy through non-Faradaic physical processes.[3] Capacitors can deliver electrical energy at high charging/discharging rates and show good long-term cycling stability, but they are limited by the low energy capacity that can be stored. Batteries, on the other hand, present high energy capacity but are limited by the low power in that this energy can be delivered. Because of the diffusion of chemical species in and out of the electrode materials during redox reactions, battery materials deteriorate quickly resulting in short cycle life. Extensive efforts have recently been made to combine the attractive characteristics of capacitors and batteries by utilizing nanomaterials as electrodes.[4] Electroactive nanomaterials are particularly attractive because of their dual functions in providing a large specific surface area (SSA) and introducing a pseudo-capacitance. These studies result in a new technology termed as electrochemical capacitors (ECs) or supercapacitors to emphasize that the specific capacitance (SC) of these materials is increased to thousands of times of those of common capacitors. Currently, there are two types of supercapacitors, that is, electrical double layer capacitors (EDLCs) and pseudo-capacitors.[5]

EDLCs store electrical charges in the electrical double layer at the electrode−electrolyte interface of a high surface area material such as highly porous activated carbons[6] or other nanostructured carbon materials.[7,8] The electrode materials only serve as a stable high-surface-area support but do not involve in redox reactions. The specific capacitance (SC) of an EDLC critically depends on both of the SSA and electrical connections of the nanomaterials. Highly porous activated carbon shows a SC as high as 125 F/g.[6] Because of the high specific surface area (up to 1500 m^2/g), high electrical conductivity (up to $\sigma = 2.5 \times 10^5\ S \cdot m^{-1}$), low mass density (~1.4 g/cm^3), high mechanical

*To whom correspondence should be addressed. E-mail: junli@ksu.edu. Fax: (785) 532-6666. Phone: (785) 532-0955.
[†] Current address: Department of Physics and Astronomy, The University of Kansas, Lawrence, KS 66045.

(1) DOE Workshop Report on Basic Research Needs for Solar Energy Utilization. 2005. http://www.sc.doe.gov/bes/reports/files/SEU_rpt.pdf.
(2) DOE Workshop Report on Basic Research Needs for Electrical Energy Storage. 2007. http://www.sc.doe.gov/bes/reports/files/EES_rpt.pdf.
(3) Winter, M.; Brodd, R. J. *Chem. Rev.* **2004**, *104*(10), 4245–4269.
(4) Arico, A. S.; Bruce, P.; Scrosati, B.; Tarascon, J. M.; Van Schalkwijk, W. *Nat. Mater.* **2005**, *4*(5), 366–377.
(5) Simon, P.; Gogotsi, Y. *Nat. Mater.* **2008**, *7*, 845–854.
(6) Gamby, J.; Taberna, P. L.; Simon, P.; Fauvarque, J. F.; Chesneau, M. *J. Power Sources* **2001**, *101*(1), 109–116.
(7) Jeong, H. K.; Jin, M.; Ra, E. J.; Sheem, K. Y.; Han, G. H.; Arepalli, S.; Lee, Y. H. *ACS Nano* **2010**, *4*(2), 1162–1166.
(8) Korenblit, Y.; Rose, M.; Kockrick, E.; Borchardt, L.; Kvit, A.; Kaskel, S.; Yushin, G. *ACS Nano* **2010**, *4*(3), 1337–1344.

 Published on Web 08/10/2010

stability (Young's modulus of ~60 to 1,000 GPa), and the ability to form interconnected networks,[9] carbon nanotubes (CNTs) have been recognized as attractive supercapacitor electrode materials. Both single-walled CNTs (SWCNTS) and multiwalled CNTs (MWCNTs) have been explored as EDLCs showing SC values varying from 4 to 135 F/g, which strongly depends on sample preparation and electric contact with the current collector as well as between CNTs.[10−12]

In contrast to EDLCs, pseudo-capacitor is an electrochemical capacitor using reversible faradaic redox reactions of a solid thin film or a layer of nanoparticles at the electrode surface.[3] Transition metal oxides are commonly used as electroactive nanomaterials. Multivalent redox reactions occur mostly at the thin surface layer to provide high reaction rates. Hydrous RuO_2 film currently represents the state of the art in pseudo-capacitor materials with the SC of 540 F/g[13] and 700 F/g.[14] However, the high cost and environmental toxicity of ruthenium limit them from practical applications. Alternatively, MnO_2 and V_2O_5 have been used as electrodes for pseudo-capacitors with reported SC values varying from 50 to 300 F/g.[15,16] Manganese oxides are particularly attractive because of the nontoxic chemical properties, low cost, and outstanding structural versatility. MnO_2 nanomaterials were synthesized using various techniques including chemical reduction, co-precipitation, sol−gel processes, thermal decomposition, and so forth.[17−22] Thin film MnO_2 electrodes were also prepared via electrochemical and chemical routes.[23,24] However, because of the low electrical conductivity, high-performance results have only been obtained with very thin (<500 nm) MnO_2 films deposited on metal electrodes, limiting the obtainable total energy capacity. Recently, we investigated a self-supported supercapacitor membrane made of entangled MnO_2 nanowires mixed with CNTs, where CNTs serve as the conductive network.[25] A maximum SC of 50 F/g was obtained at 80 wt % of MnO_2 nanowires. As more MnO_2 nanowires are incorporated, the redox activity of MnO_2 quickly decreases because of poor electrical connection between CNTs and low-conductivity MnO_2 nanowires.

Ideally, the connection issue can be solved by directly depositing MnO_2 onto an active nanostructured electrode.[16] This creates a hybrid supercapacitor with a large pseudocapacitance in addition to the high capacitance provided by the electrical double layer at the supporting electrode surface. Vertically aligned CNTs directly grown on conductive substrates provide a potential solution for both large active surface area and good electrical connection. Zhang et al. recently demonstrated that MnO_2 nanoclusters can be electrodeposited on a dense vertically aligned CNT array and showed a SC value of 199 F/g.[26] Reddy et al. further showed that MnO_2 can be coaxially coated on CNTs in a filtration membrane and used as a storage medium for Li-ion batteries.[27] Here we report on the use of a 4 μm tall brush-like carbon structure directly grown on a conductive surface, that is, vertically aligned carbon nanofiber (VACNF) array, as a three-dimensional (3D) nanostructured template to support coating of a uniform MnO_2 film by a unique cathodic electrodeposition method. The open interfiber spacing (~300 nm) and small MnO_2 thickness (~2−15 nm) enable fast electrolyte access and high redox reaction rate. Such coaxially coated hybrid supercapacitors give a remarkable SC value of 365 F/g. The specific energy, specific power, and cycle stability have all been significantly improved compared to bulk MnO_2 materials.

Experimental Section

VACNF arrays were grown on ~1×2 cm^2 Si substrates coated with 100 nm thick Cr using a DC-biased plasma enhanced chemical vapor deposition (PECVD) system (AIXTRON) at ~800 °C following previously published procedures.[28−31] A 22 nm thick Ni film was used as the catalyst, and a mixture of C_2H_2 (at 62 sccm) and NH_3 (at 252 sccm) was used as the gas precursors at a processing pressure of ~4.12 Torr. The VACNF samples used in this study have an tunable average diameter of ~50−150 nm, a fixed average density of ~1×10^9 CNFs/cm^2, and a fixed average length of ~4 μm controlled by 20 min of growth time. Some VACNFs were directly used, but others were pretreated in 1.0 HNO_3 for 5−10 min before electrochemical experiments. Once the VACNF array was subjected to a wet process, it was always kept in wet conditions until all studies were completed. The transferring of the wet VACNF arrays in the air was minimized to avoid drying up; that was known to cause VACNF arrays collapsing into microbundles by the capillary force.[32]

(9) Meyyappan, M. *Carbon Nanotubes Science and Applications*; CRC Press: Boca Raton, FL, 2004.
(10) Frackowiak, E.; Metenier, K.; Bertagna, V.; Beguin, F. *Appl. Phys. Lett*. **2000**, *77*(15), 2421–2423.
(11) Kaempgen, M. C.; Chan., C. K.; Ma, J.; Cui, Y.; Gruner, G. *Nano Lett*. **2009**, *9*(5), 1872–1876.
(12) Liu, C. G.; Liu, M.; Li, F.; Cheng, H. M. *Appl. Phys. Lett*. **2008**, *92* (14), 143108.
(13) Chang, K. H.; Hu, C. C.; Chou, C. Y. *Chem. Mater*. **2007**, *19*(8), 2112–2119.
(14) Zheng, J. P.; Cygan, P. J.; Jow, T. R. *J. Electrochem. Soc*. **1995**, *142*(8), 2699–2703.
(15) Broughton, J. N.; Brett, M. J. *Electrochim. Acta* **2005**, *50*(24), 4814–4819.
(16) Fischer, A. E.; Pettigrew, K. A.; Rolison, D. R.; Stroud, R. M.; Long, J. W. *Nano Lett*. **2007**, *7*(2), 281–286.
(17) Jeong, Y. U.; Manthiram, A. *J. Electrochem. Soc*. **2002**, *149*(11), A1419–A1422.
(18) Kim, H.; Popov, B. N. *J. Electrochem. Soc*. **2003**, *150*(3), D56–D62.
(19) Reddy, R. N.; Reddy, R. G. *J. Power Sources* **2003**, *124*(1), 330–337.
(20) Reddy, R. N.; Reddy, R. G. *J. Power Sources* **2004**, *132*(1−2), 315–320.
(21) Toupin, M.; Brousse, T.; Belanger, D. *Chem. Mater*. **2002**, *14*(9), 3946–3952.
(22) Toupin, M.; Brousse, T.; Belanger, D. *Chem. Mater*. **2004**, *16*(16), 3184–3190.
(23) Hu, C. C.; Tsou, T. W. *Electrochem. Commun*. **2002**, *4*(2), 105–109.
(24) Pang, S. C.; Anderson, M. A. *J. Mater. Res*. **2000**, *15*(10), 2096–2106.
(25) Fang, Y.; Liu, J.; Li, J. *J. Nanosci. Nanotechnol*. **2010**, *10*, 5099−5105.
(26) Zhang, H.; Cao, G. P.; Wang, Z. Y.; Yang, Y. S.; Shi, Z. J.; Gu, Z. N. *Nano Lett*. **2008**, *8*(9), 2664–2668.
(27) Reddy, A. L. M.; Shaijumon, M. M.; Gowda, S. R.; Ajayan, P. M. *Nano Lett*. **2009**, *9*(3), 1002–1006.
(28) Cruden, B. A.; Cassell, A. M.; Ye, Q.; Meyyappan, M. *J. Appl. Phys*. **2003**, *94*, 4070.
(29) Haque, M. S.; Teo, K. B. K.; Rupensinghe, N. L.; Ali, S. Z.; Haneef, I.; Maeng, S.; Park, J.; Udrea, F.; Milne, A. I. *Nanotechnology* **2008**, *19*(2), 5.
(30) Melechko, A. V.; Merkulov, V. I.; McKnight, T. E.; Guillorn, M. A.; Klein, K. L.; Lowndes, D. H.; Simpson, M. L. *J. Appl. Phys*. **2005**, *97*(4), 41301−1–41301−39.
(31) Ren, Z. F.; Huang, Z. P.; Xu, J. W.; Wang, J. H.; Bush, P.; Siegal, M. P.; Provencio, P. N. *Science* **1998**, *282*, 1105–1107.
(32) Nguyen-Vu, T. B.; Hua, C.; Alan, C.; Russell, A.; Meyya, M.; Jun, L. *Small* **2006**, *2*(1), 89–94.

An O-ring with ~4 mm i.d. was used to define the surface area that was exposed to the solution confined in a Teflon cell. A potentiostat (Parstat 2273 Analyzer, Princeton Applied Research Corporation) was used to control the experiments using a three-electrode setup. The working electrodes were the VACNF arrays described above. A Pt coil and a Ag/AgCl(sat'd KCl) electrode were used as the counter electrode and reference electrode, respectively. Electrochemical deposition of MnO_2 was obtained with a pulsed potentioamperometric method in aqueous solutions containing 0.050 M Manganese(II) acetate and 0.10 M Na_2SO_4 (pH = 6.92). Manganese(II) acetate, sodium sulfate, and potassium chloride were purchased from Thermo Fisher Scientific Inc. The electrode potential was stepped to −0.30 V (vs Ag/AgCl(sat'd KCl)) for 60 s to initiate Mn deposition and then stepped to open circuit potential for ~120 s to allow Mn^{2+} ions diffusing into the VACNF array. This waveform was repeated until the desired total amount of Mn is deposited and the total deposition time is added up to indicate the deposition quantity. A mixture of manganese oxides were formed and remained stable when the working electrode is returned to the open circuit potential after the deposition. The average oxidation state of the Mn on CNTs was presumed to be 3.45, that is, in form of a mixture of MnO_2 and Mn_3O_4, as determined by XPS in a previous report.[26] Many other studies simply refer the deposited manganese oxide as MnO_2 since it is the dominant form.[15,20,27] To simplify it, we use manganese oxide or MnO_2 in this paper to refer to the electrochemically deposited manganese material on the VACNF arrays.

Potentiostatic cyclic voltammetry (CV) and galvanostatic Chronopotentiometry (CP) measurements were carried out to characterize the VACNFs before and after manganese oxide coating during charge−discharge cycles in 0.10 M Na_2SO_4. CV measurements were carried out in the potential range of −0.10 to +0.80 V (vs Ag/AgCl (sat'd KCl)) at various scan rates from 50 to 5000 mV/s. CP charge−discharge measurements were carried out at fixed current density varying from 0.05 to 2.0 mA/cm^2 in each experiment. Electrochemical impedance spectra were measured with a sinusoidal wave of 10.0 mV amplitude at the open circuit potential in 0.10 M Na_2SO_4 aqueous solution with frequencies spanned from 100 kHz and 0.1 Hz.

The structure of the VACNF samples and manganese oxide coating was routinely examined with scanning electron microscopy (SEM; Hitachi VP-SEM S-3400N and Leo 1550 FESEM) and transmission electron microscopy (TEM; FEI CM100).

Results and Discussion

The processes to fabricate the hybrid supercapacitor are schematically shown in Figure 1a. First, a Cr layer with thickness of 100 nm was coated on the Si substrate as the conductive film, and then a Ni layer of 22 nm in thickness was deposited as the catalyst. Second, VACNF arrays were grown by DC-biased plasma enhanced chemical vapor deposition (PECVD). Third, according to specific experiment design, some samples were treated in 1.0 M HNO_3 solution. Fourth, a thin layer of manganese oxide was deposited on the surface of VACNFs using an electrochemical method. The average oxidation state of manganese in the deposited film at open circuit potential is presumed to be about 3.45, similar to that in a previous study of MnO_2 nanoflowers deposited on CNTs which was determined by X-ray photoelectron spectroscopy (XPS).[26] To simplify it, we refer to it as manganese oxide in this paper. In some discussions, it is simply called as MnO_2 since MnO_2 is the dominant form.

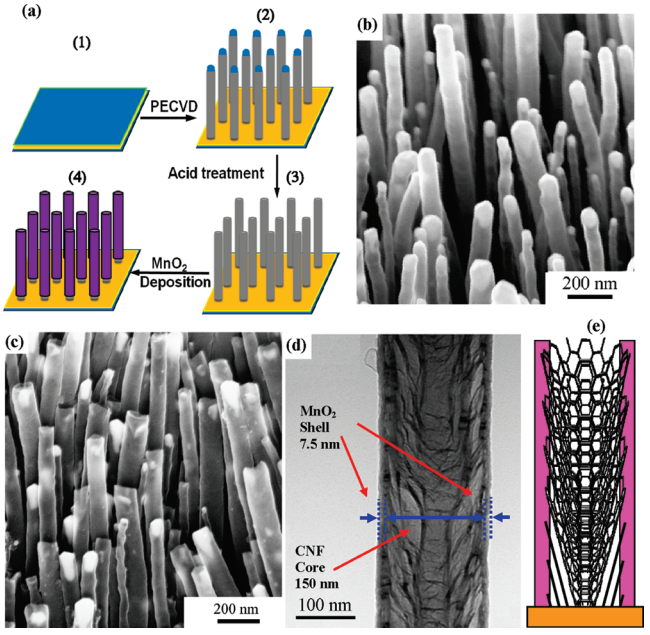

Figure 1. (a) Schematic of the fabrication processes of the hybrid supercapacitors by coating a uniform manganese oxide layer on the vertically aligned carbon nanofiber array. (b) A SEM image at 45° perspective view of an as-grown vertically aligned carbon nanofiber array. (c) A SEM image at 45° perspective view of a vertically aligned carbon nanofiber array after 10−15 min of treatment in 1.0 M HNO_3 followed by 20 min of electrochemical deposition to coat manganese oxide. (d) A TEM image of the same sample as that in (c), indicating the uniform coating of ~7.5 nm manganese oxide layer on the 150 diameter carbon nanofiber, presumably dominated by MnO_2. (e) Schematic illustration of the uniform MnO_2 coating on the sidewall of the cup-stacking graphitic structure of carbon nanofibers, likely associated with the active broken graphitic edges.

Figure 1b shows the SEM image of an as-grown VACNF array, in which each CNF free-stands on the substrate surface with a Ni catalyst particle present at the tip. The average diameter of the CNFs in this particular sample is ~150 nm, but it can be controlled from 50 to 150 nm in our study. VACNF arrays with smaller diameters (less than 80 nm) are expected to give a larger surface to volume ratio while those with larger diameter (larger than 100 nm) give much stronger mechanical properties. An average diameter of 150 nm is chosen for this study since the vertical array structure is robust and can be retained through many solution processes. VACNF arrays with smaller average diameter (less than 80 nm) or longer length (more than 5 μm) tend to collapse into microbundles by capillary force during the drying process after they are taken out of solutions.[32] Even though this can be solved by keeping the VACNF sample always submerged in solutions or using supercritical fluid drying when taking out from solutions, we avoid such complication by using robust VACNFs with large diameter and short length to demonstrate the principle. The structure of VACNF arrays can be optimized in future studies to enhance the performance. The average length of all VACNF samples is controlled at 4 μm, giving at least ~27:1 aspect ratio in our study. The well-defined vertical alignment and the large open space (~300 nm average nearest-neighbor distance) make VACNF arrays distinct from other "vertical aligned CNTs" in the literature in which CNTs have much higher density, smaller diameter (<20 nm), and heavily

entangled matt-like structure.[26] The 3D nanobrush structure of VACNF array enables the electrolyte to easily access the entire surface of all CNFs and thus produces uniform manganese oxide deposition and fast redox kinetics.

Figure 1c shows the SEM image of an acid-treated VACNF array after depositing manganese oxide at −0.30 V (vs Ag/AgCl(sat'd KCl)) from 0.05 M manganese(II) acetate for 20 min. A thin layer of manganese oxide uniformly wraps around each CNF. The VACNF array nicely retains its original vertical alignment. The coating is so thin and uniform that one cannot unambiguously determine the deposition with SEM images. However, the Ni catalyst particles at the CNF tip were clearly removed by the acid treatment. Further analysis was done by TEM to understand the manganese oxide deposition. A TEM image of the same sample is shown in Figure 1d which reveals that the manganese oxide layer is only 5−10 nm in thickness. Furthermore, we can measure the statistical diameter distribution of the VACNFs before and after MnO_2 deposition using SEM images shown in Figure 1b and 1c. The diameter distributions are fit with Gaussian curves (see Supporting Information, Figure S1) with the mean value and standard deviation as $d_0 = 150 \pm 42.6$ nm for as-grown CNFs and $d_1 = 165 \pm 35.2$ nm after manganese oxide deposition. The derived average thickness of the manganese oxide coating is ~7.5 nm, very consistent with the TEM measurement.

The cathodic electrochemical deposition of MnO_2-dominated manganese oxide material at a negative potential, such as −0.30 V versus Ag/AgCl(sat'd KCl) in this study, is a very interesting new phenomenon. Intuitively, one would think that an anodic deposition using a positive potential is required so that the starting Mn(II) species can be oxidized into Mn(IV) and deposited as MnO_2. Indeed, most previous studies on electrochemical deposition of MnO_2 used cyclic voltammetry (CV) in the potential range from around the open circuit potential to a high positive potential such as 1.2 V[26] or 0.90 V[33] (vs Saturated Calomel Electrode (SCE)). However, we found that the anodic deposition only produced sparse MnO_2 nanoparticles on the VACNF arrays, similar to the SEM images shown in Supporting Information, Figure S2. But it was not successful to fabricate a uniform MnO_2 coating. To solve this problem, we tried cathodic deposition with negative potentials, originally in an attempt to reduce Mn^{2+} to Mn(0) and then oxidize it into MnO_2 by another method. To our surprise, only a small potential window around −0.30 V (vs Ag/AgCl(sat's KCl)) works well. An ultrathin but uniform MnO_2 layer can be deposited on VACNFs which is confirmed by both electron microscopy and electrochemical characterization.

The deposition mechanism likely involves the combination of two processes, that is, the electrolysis of water and electrochemical oxidation of Mn(II). In recent studies,[34,35] Liu et al demonstrated that mesoporous hydrous manganese dioxide nanowall arrays can be cathodically deposited on Pt films at a large negative potential ranging from −1.2 to −2.2 V. They attribute the cathodic MnO_2 deposition to water electrolysis induced co-precipitation. According to this mechanism, the large negative potential induces electrolysis of water into hydrogen gas and causes the pH value in the vicinity of the cathode to increase to a much higher level, which then results in the precipitation of manganese(II) hydroxide $Mn(OH)_2$. Since $Mn(OH)_2$ is not stable in the presence of oxygen, it is readily oxidized to a mixture of Mn_3O_4 and MnO_2 after drying in the air. In our study, however, the applied potential (i.e., −0.30 V vs Ag/AgCl(sat'd KCl)) is much higher than the potential range employed by Liu et al.[34,35] and only induces mild electrolysis. In addition, the sample after manganese oxide deposition was always kept in wet conditions and was quickly transferred into 0.10 M $NaSO_4$ for electrochemical characterization. The possibility to oxidize $Mn(OH)_2$ deposits into MnO_2 seems low.

However, a water electrolysis induced electrochemical oxidation may explain the results. There are two possible oxidation reactions:

$$Mn^{2+} + 4H_2O \leftrightarrow MnO_2(s) + 4H^+ \quad (1)$$

$$3Mn(OH)_2(s) + 2OH^- \leftrightarrow Mn_3O_4(s) + 4H_2O + 2e^- \quad (2)$$

The standard reduction potentials for these two reactions are 1.230 V and −0.352 V versus standard hydrogen electrode (SHE), respectively.[36] The actual reduction potentials are pH dependent and can be calculated by the Nernst equation. At pH = 7, the reduction potentials are 0.245 V and −0.136 V versus Ag/AgCl(sat'd KCl), both of which are much higher than the applied potential (−0.30 V) in our electrochemical deposition process. As a result, no direct electrochemical oxidation will occur. However, the mild water electrolysis at −0.30 V may be sufficient to induce the change in pH value at the VACNF surface. The porous 3D nanostructure of VACNF array may make this change bigger than on a flat surface by retaining the produced OH^- ions inside the electrode. If the pH value increases to 12, then the reduction potentials for eqs 1 and 2 will drop to −0.345 V and −0.431 V, respectively, both below −0.30 V. At this condition, Mn(II) can be electrochemically oxidized into MnO_2 or Mn_3O_4 solids. This will form a uniform manganese oxide coating instead of the mesoporous nanowall structure in Liu's studies.[34,35] While the exact mechanism may need extensive studies, the above mechanism is sufficient to guide us in preparing samples for energy storage study.

The sidewall of CNTs has poor electrochemical activity because of the structural similarity to graphite basal plan. This may be a part of the reason that only sparse manganese oxide clusters were obtained by electrochemical deposition on MWCNT arrays in the study by Zhang et al.[26] The PECVD-grown VACNF used in this study has a

(33) Wu, M. S. Appl. Phys. Lett. **2005**, *87*, (15).
(34) Liu, D.; Garcia, B. B.; Zhang, Q.; Guo, Q.; Zhang, Y.; Sepehri, S.; Cao, G. *Adv. Funct. Mater.* **2009**, *19*(7), 1015–1023.
(35) Liu, D.; Zhang, Q.; Xiao, P.; Garcia, B. B.; Guo, Q.; Champion, R.; Cao, G. *Chem. Mater.* **2008**, *20*(4), 1376–1380.
(36) Harris, D. C. *Quantitative Chemical Analysis*, 7th ed.; W. H. Freeman and Company: New York, 2007.

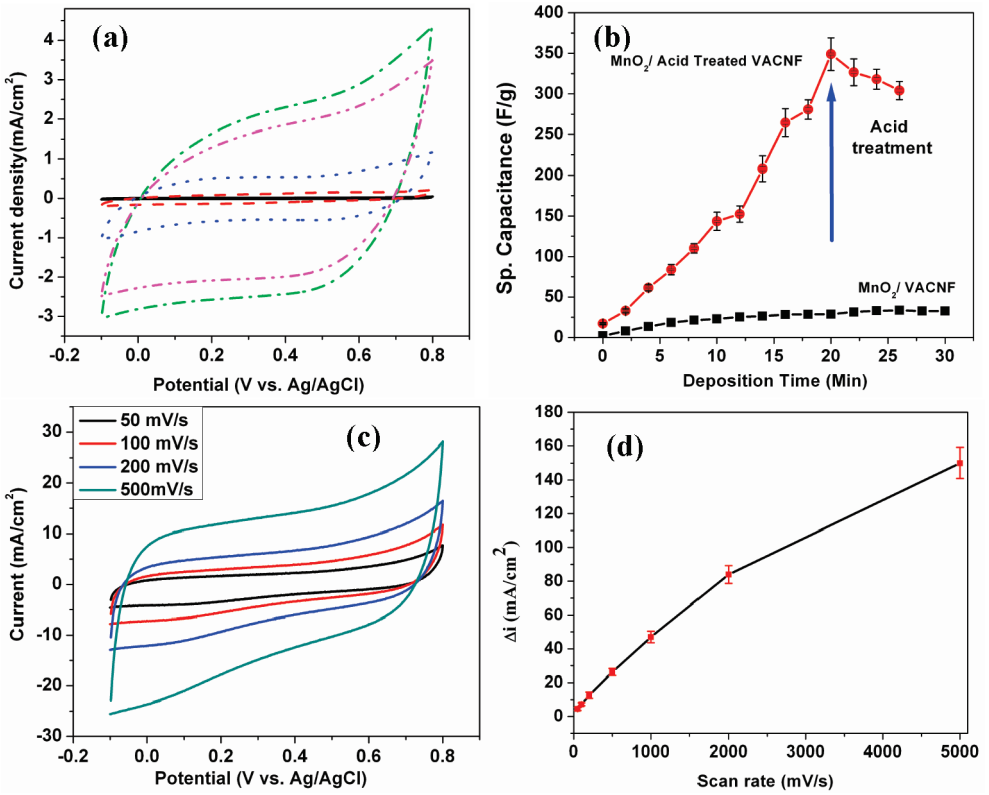

Figure 2. (a) Cyclic voltammograms of an acid-treated VACNF array measured at a scan rate of 50 mV/s in 0.10 M Na_2SO_4 at various MnO_2 deposition time: untreated VACNF (black solid line), acid-treated VACNF (red dashed line), and acid-treated VACNFs with manganese oxide deposition for 6 min (blue dotted line), 20 min (purple dash-dot-dot line) and 26 min (green dash-dot line); (b) the specific capacitance of an untreated VACNF array and an acid-treated VACNF calculated from the cyclic voltammograms versus the total manganese oxide deposition time; (c) cyclic voltammograms at various scan rates measured with the acid-treated VACNF array after 20 min of manganese oxide deposition; and (d) the separation between the anodic and cathodic currents (i.e., Δi) at 0.30 V (vs Ag/AgCl (sat'd KCl) in cyclic voltammograms measured at various scan rates.

unique structure consisting of cup-like graphitic cones stacking along the fiber axis,[30,31,37] as schematically shown in Figure 1e. As a result, it presents a series of broken graphitic edges which are very active sites similar to graphite edge plan electrodes. This may be another reason that we were able to deposit a uniform manganese oxide coating covering the entire sidewall of CNFs. The redox reaction rate of the manganese oxide coating is also expected to be very high, leading to high-performance pseudo-capacitors.

The surface property is critical in defining the electrochemical activity of carbon materials. We found that only sparse manganese oxide nanoparticles can be deposited on the as-grown VACNFs (see Supporting Information, Figure S2). This is likely due to the thin layer of amorphous carbon formed on the CNF surface during PECVD growth process. Acid treatment effectively activated the CNF surface by removing the amorphous carbon, creating oxide groups, and exposing the active graphitic edges. As a result, the amount of active manganese oxide that can be deposited on the CNF surface is dramatically increased.

Figure 2a shows CV curves of an acid-treated VACNF array after coating with various amount of manganese oxide. The SC (C_0) of the electrode is proportional to the sum of the integrated charges of anodic and cathodic cycle, that is, $(Q_a + |Q_c|)$, as given by

$$C_0 = (Q_a + |Q_c|)/(2m\,\Delta V) \tag{3}$$

where m is the total mass of the CNF and manganese oxide and $\Delta V = 0.90$ V for potential window between −0.10 to +0.80 V (vs Ag/AgCl (sat'd KCl)). The CNFs are randomly distributed with an average density of $\sim 1 \times 10^9$ CNFs/cm^2. The mass of the VACNF array is estimated to be 1.06×10^{-4} g/cm^2 by assuming CNFs as solid nanowires with an average diameter of 150 nm, area density of 1×10^9 CNFs/cm^2, length of 4 μm, and a mass density similar to commercial graphite at 1.7 g/cm^3.[38] The mass of the 7.5 nm thick MnO_2 coating on the VACNF array is ~2.4 x10^{-5} g/cm^2 by assuming the density of electrochemically deposited manganese oxide as MnO_2 with a mass density of 1.65 g/cm^3.[39] The sum of charge is extracted from the CV profile (cyclic voltammograms) by integrating around the $I(V)$ loops[40]

$$Q_a + |Q_c| = \int_{-0.1V}^{0.8V} \frac{I(V)}{v}\,\mathrm{d}V \tag{4}$$

(37) Ngo, Q.; Yamada, T.; Suzuki, M.; Ominami, Y.; Cassell, A. M.; Li, J.; Meyyappan, M.; Yang, C. Y. *IEEE Trans. Nanotechnol.* **2007**, *6* (6), 688–95.

(38) Sato, Y.; Ootsubo, M.; Yamamoto, G.; Van Lier, G.; Terrones, M.; Hashiguchi, S.; Kimura, H.; Okubo, A.; Motomiya, K.; Jeyadevan, B.; Hashida, T.; Tohji, K. *ACS Nano* **2008**, *2*(2), 348–356.

(39) Demishima, B. A. L.; Ohtsuka, T.; Konno, H.; Sato, N. *Electrochim. Acta* **1991**, *36*(9), 1485–1489.

(40) Fang, Y.; Liu, J.; Yu, D. J.; Wicksted, J. P.; Kalkan, K.; Topal, O.; Flanders, B. N.; Wu, J.; Li, J. *J. Power Sources* **2010**, *195*(2), 674–679.

where the potential scan rate is $v = 50$ mV/s. The charge−discharge current initially increases as more manganese oxide is deposited, indicating the contribution of pseudo-capacitance. It reaches a maximum at ~20−30 min of deposition and then decreases. The as-grown VACNF has a SC value of ~2.5 F/g (Supporting Information, Figure S3a). After MnO_2 deposition for 26 min, the SC value increases to the maximum at 36 F/g. With a pretreatment in 1.0 M HNO_3 for 5−10 min, the SC value of the bare VACNF array was dramatically increased to 23 F/g (Supporting Information, Figure S3b), over 9 times of the untreated one. This effect is consistent with the TEM/SEM images in Figure 1 and Supporting Information Figure S2) and a previous study.[32] Figure 2b shows the SC value calculated from the CV measurements according to eqs 3 and 4, a remarkable maximum value of 349 F/g was obtained with the acid-treated VACNF array after 20 min of manganese oxide deposition. The decrease in SC value as more manganese oxide is deposited can be attributed to the decrease in electrical connection and slowing down of mass transport as the layer thickness increases.

Figure 2c shows CV measurements at various scan rates from 50 to 500 mV/s obtained with an acid-treated VACNF after 20 min of manganese oxide deposition (i.e., at the maximum of Figure 2b). The CV curves are nearly rectangular, indicating fast charging/discharging processes. For an ideal capacitor, the charging/discharging current quickly rises up when the scan direction is reversed at the potential limit and reaches a leveled value. Thus nearly rectangular CV profiles with sharp corners are expected. The manganese oxide-coated VACNF array involves redox reactions during the potential cycle producing anodic/cathodic currents as Mn atoms in the overlayer is converted into higher/lower valence states. This surface redox reaction leads to the pseudo-capacitance, behaving similar to normal capacitance. The separation between leveled anodic and cathodic currents (Δi) is linearly proportional to the capacitance C and CV scan rate (v) as follows:

$$\Delta i = 2C \times v \tag{5}$$

Figure 2d shows the value of Δi at 0.30 V (vs Ag/AgCl-(sat'd KCl)) from CV curves at various scan rates. Clearly, it lineally increases with the scan rate v up to 2000 mV/s, which is significantly higher than those used in other pseudo-capacitance studies such as MnO_2 on CNTs (at 1−200 mV/s)[25,26,41] and polypyrrole on CNTs (1−100 mV/s).[40,42,43] This indicates that the thin conformal manganese oxide coating on VACNF array can provide much higher specific power attributed to the fast redox reactions. At the scan rate of over 2000 mV/s, the curve starts to deviate from the straight line, indicating that the power, that is, the rate to release the electrical energy, is limited by the reaction rate.

To further investigate the specific power, a set of charge−discharge experiments were carried out with chronopotentiometry (CP) in galvanostatic mode with an acid-treated VACNF array after 20 min of manganese oxide deposition as shown in Figure 3a. The curves are nearly linear and symmetric at a charging/discharging current of $I_0 = 0.3$ mA/cm^2 (i.e., ~2.3 A/g), which implies that the electrode has excellent electrochemical reversibility and rapid charge−discharge properties. The SC value C_0 can be calculated according to the following equation:[9]

$$C_0 = \frac{I \times t}{\Delta V \times m} \tag{6}$$

where I is the current density during charging/discharging process, t is the charge−discharge time in each segment, ΔV is the potential window set in the experiment (i.e., 0.80 V in this study with the low limit at 0.0 V and the high limit at 0.80 V), and m is the total mass of CNF and manganese oxide. The obtained value is 318 F/g, close to ~349 F/g calculated from CV measurements. We continuously repeated the charge−discharge for 500 cycles. The curves of the initial 4 cycles are plotted in Figure 3a, which do not show any noticeable change. The SC values after every 50 cycles are calculated and shown in Figure 3b. The MnO_2/VACNF electrode shows remarkable stability over the cycling, with the value only decreased by ~11% to 283 F/g after 500 cycles. However, CV curves measured at a slow scan rate of 50 mV/s at the original state and after the 500th cycle, as shown in Figure 3c, are almost completely overlapped, indicating that the change in the quantity of manganese oxide coating is minimum. The decrease in the SC value may be simply attributed to the heating effect after long charging-discharging cycles or other physical factors rather than irreversible chemical or structural changes with the electrode materials. The results from CV and galvanostatic charging-discharging measurements consistently validated the remarkable SC and excellent cycle stability.

The two important parameters measuring the performance of an EES device, that is, the specific energy (E_0) and specific power (P_0), are calculated by following equations:

$$E_0 = \frac{1}{2} C_0 (\Delta V)^2 \tag{7}$$

$$P_0 = \frac{(\Delta V)^2}{4 \times \mathrm{ESR}} \tag{8}$$

where ESR is the equivalent series resistance which represents the total internal resistance of the electrochemical cell. The magnitude of both C_0 and ESR depends on the charging-discharging current density. As shown in Figure 4a, the gravimetric SC, that is, C_0, of a manganese oxide-coated VACNF array is 365 F/g at the charge−discharge current density of 0.050 mA/cm^2 (i.e., ~0.385 A/g). This value decreases to ~70 F/g as the current density is increased to 2.0 mA/cm^2 (i.e., ~15 A/g), indicating the decrease of E_0. In the meantime, ESR decreases with the current density, which is measured from the drop in cell

(41) Fan, Z.; Chen, J. H.; Wang, M. Y.; Cui, K. Z.; Zhou, H. H.; Kuang, W. *Diamond Relat. Mater.* **2006**, *15*(9), 1478–1483.
(42) Khomenko, V.; Frackowiak, E.; Beguin, F. *Electrochim. Acta* **2005**, *50*(12), 2499–2506.
(43) Gupta, V.; Norio, M. *Electrochim. Acta* **2006**, *52*(4), 1721–1726.

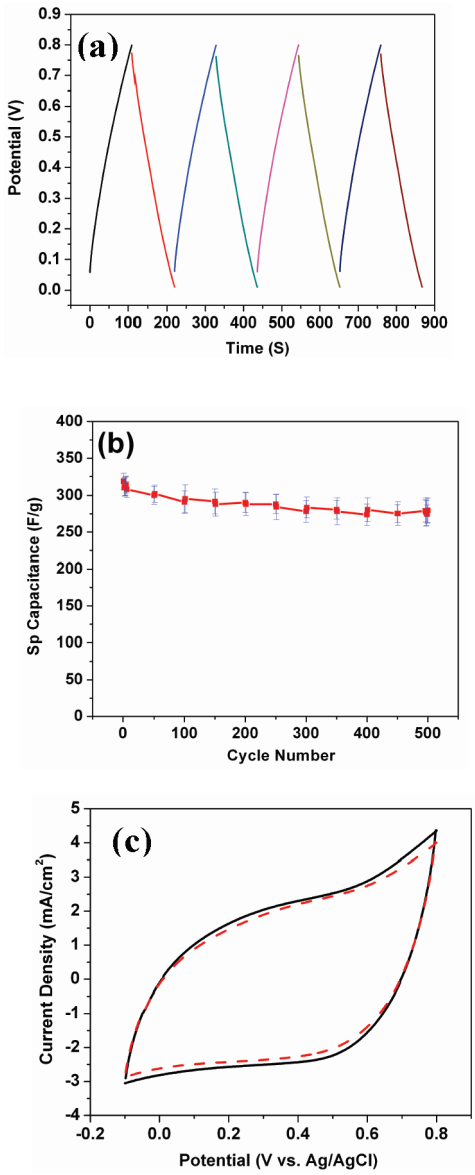

Figure 3. (a) First 4 cycles of galvanostatic charge−discharge curves of an acid-treated VACNF array after 20 min of manganese oxide deposition in 0.10 M Na_2SO_4 aqueous solution measured with chronopotentiometry at a charging/discharging current of 0.3 mA/cm^2. (b) The specific capacitance as a function of the cycle number. (c) The cyclic voltammograms of the same VACNF array before the first charge−discharge cycle (black solid line) and after 500 cycles (red dashed line) at a scan rate of 50 mV/s.

voltage as the polarity of the charge−discharge current is reversed at the cell voltage limits. Accordingly, the obtained specific power P_0 increases until a maximum charge-discharging current density is reached. Figure 4b illustrates the relationship between the estimated values of E_0 and P_0 at various charge−discharge rates for an EES device that may be made with MnO_2−VACNF electrodes with 0.80 V of cell voltage. The specific energy E_0 decreases from 32.5 to 6.2 W h/kg, and the specific power increases from 3620 to 6216 W/kg as the charge−discharge current increased from 0.050 to 2.0 mA/cm^2 (i.e., ~0.385 to 15 A/g).

In calculating the value of E_0 and P_0 in Figure 4b, we include the estimated mass of CNF support and manganese

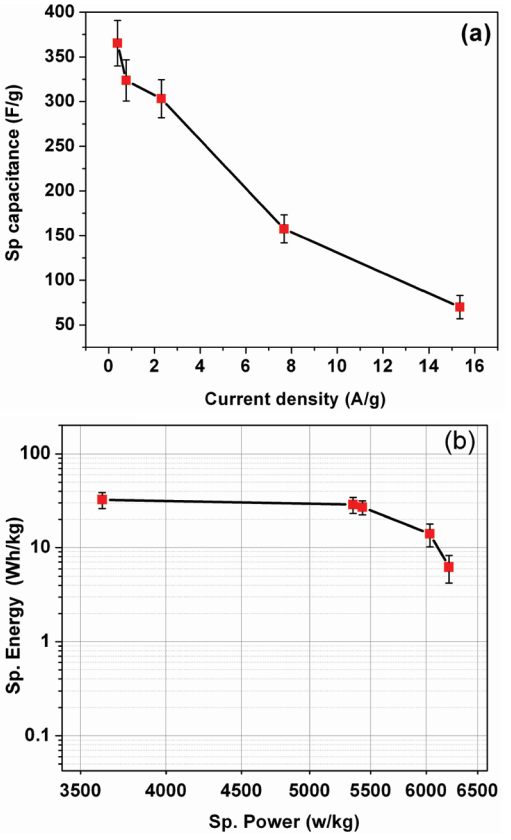

Figure 4. (a) Specific capacitance of the 20 min deposited VACNF array as a function of the charge−discharge current density. (b) Ragone plot of the estimated specific energy and specific power at various charge−discharge rates (i.e., current densities).

oxide for the purpose to compare with the materials properties in the literature[15,41,44] in which the mass of current collector and/or substrate were normally neglected. For practical EES applications, VACNF arrays can be grown on 10 μm thick Cu foils, and the length of CNFs can be increased to over 20 μm to maximize the mass ratio of the active electrode materials to the substrate. The growth of such materials has been demonstrated in our lab (data not included). The Cu foil has an area density of ~8.9×10^{-3} g/cm^2, which is about 13.6 times of the sum of CNF and MnO_2 on a 20 μm high VACNF (i.e., ~6.5×10^{-4} g/cm^2). The value of E_0 and P_0 would be reduced for such practical EES devices. Optimization of materials assembly and device design is needed to fully realize the potential high performance of manganese oxide-coated VACNF array that is revealed by this study.

The mechanism of energy storage in manganese oxide involves varying the valence states of some Mn atoms during the charge/discharge processes.[22] The mole number of the deposited Mn can be estimated from the film thickness obtained by SEM and TEM measurements, which is about 2.76×10^{-7} mol/cm^2 by assuming that they are present in the form of MnO_2 with a density of 1.65 g/cm^3. On the other hand, the integrated anodic charge Q_a or cathodic charge Q_c indicates that 6.18×10^{-8} mol/cm^2 of

(44) Reddy, A. L. M.; Ramaprabhu, S. *J. Phys. Chem. C* **2007**, *111*(21), 7727–7734.

electrons are involved in each charge−discharge process between −0.10 to 0.80 V, that is, only an average of ~0.22e per Mn is involved in each process. This can be also viewed as that only 22% of manganese oxide is involved in the one-electron redox reactions. If the average oxidation state of Mn (in form of a mixture of MnO_2 and Mn_3O_4) is about 3.45 (as determined by XPS in a previous study[26]), it only changes from 3.34 to 3.56 in each charging or discharging process. Clearly, only a small portion of the energy storage capacity is employed under our measurement conditions. There is still a large room for further improvement by having more Mn atoms involved in the reaction.

To further understand the charge transfer, electrochemical kinetics, and internal resistances that influence the supercapacitor performance, we carried out electrochemical impedance spectroscopy (EIS) measurements in the same setup as the CV and CP studies. Figures 5a and 5b show Nyquist plots of the EIS spectrum of an acid-treated VACNF array before and after manganese oxide deposition, which are measured over a frequency range from 100 kHz to 0.1 Hz. The data of the bare VACNF sample can be nicely fit with an equivalent circuit consisting of a serial resistor R_s attributed to solution resistance in connection with a parallel circuit consisting of a constant phase element (CPE) to account for the double-layer capacitance and a charge-transfer resistance (R_{ct}) in series with a capacitor C to account for the pseudo-capacitance by a small amount of redox oxygen-containing groups at the CNF surface. The fitting parameters are listed in the Supporting Information, Table SI. A CPE deviates from a pure capacitor because of the inhomogeneous electrode surface activity, with the impedance Z_{CPE} defined as

$$Z_{CPE} = 1/(Yi\omega)^{\alpha} \quad (9)$$

where ω is the angular frequency ($\omega = 2\pi f$); f is the conventional frequency in hertz; Y and α are fitting parameters. The fit value of α is 0.8119 for the EIS data in Figure 5a. After manganese oxide deposition, both the imaginary and real parts of the impedance in the EIS are dramatically reduced as shown in Figure 5b. The data can be fit with the same equivalent circuit as that before manganese oxide deposition. The R_s values of the acid treated VACNF array and those after 6 and 20 min of manganese oxide deposition are 306.6, 335.5, and 319.1 Ohm, respectively, which are almost the same. This is consistent with the fact that R_s is attributed to the solution resistance of the electrolyte and is insensitive to the condition of the electrode surface. Both of the pseudo-capacitance and CPE's Y value increase as more manganese oxide is deposited. The charge-transfer resistance R_{ct} jumps up from 28.78 Ohm to 202.6 Ohm when manganese oxide is deposited for 6 min but then decreases to 154.6 after 20 min of deposition. The EIS measurements on untreated VACNF arrays show mostly the similar trend. Overall, the EIS results indicate that the manganese oxide-coated VACNF array contributes both a fast pseudo-capacitance and the EDLC (in form of a CPE). Since the EIS measurements were done at the equilibrated open circuit potential, they are not intended for direct quantitative comparison with CV and CP measurements which were carried out in non-equilibrium conditions. The phase angle also changes after MnO_2 deposition. The alternating current (AC) signal of acid-treated VACNF is mostly in-phase with the voltage bias at frequencies over 20 Hz but monotonically changes to −70 at lower frequencies (see Supporting Information, Figure S5). As more MnO_2 is coated, the in-phase characteristic extends to ~3 Hz. For VACNFs without acid treatment, the phase angle starts to increase at two to three times higher frequencies.

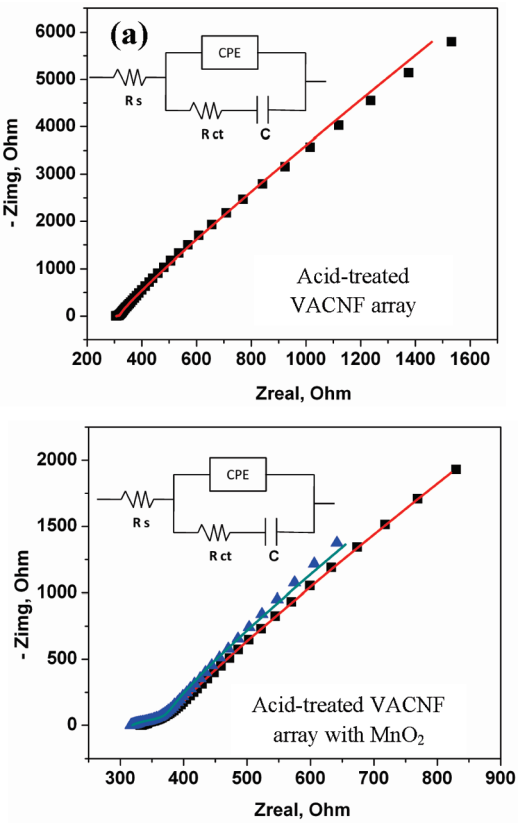

Figure 5. Nyquist plot of the electrochemical impedance spectrum and the fitting curve (solid lines) based on the inset equivalent circuit models with a bare acid-treated VACNF array (a), and that after 6 min (black filled square) and 20 min (blue filled triangle) of manganese oxide deposition (b).

Conclusions

In conclusion, we have demonstrated the fabrication of hybrid supercapacitor electrodes based on coaxially coating manganese oxide on a vertically aligned carbon nanofiber array. The cathodic deposition of manganese oxide from a neutral Mn(II) solution is likely based on the combination of water electrolysis and electrochemical oxidation at −0.30 V versus Ag/AgCl(sat'd KCl). The former process causes the increase of the pH value at the electrode surface from ~7 to 11−13 and enables the oxidation of Mn(II) to MnO_2. A uniform manganese oxide layer dominated by MnO_2 can be uniformly deposited around each CNF. This unique core-shell nanostructure with a large effective surface area (more than 10 times higher

than a flat surface) offers a highly conductive and robust core for reliable electrical connection to the MnO_2 shell, which ensures the fast redox reaction kinetics and easy electrolyte access to a large volume of active electrode materials. These factors enhance the charge transfer rate and total specific capacitance. The pseudo-capacitance of 313 F/g in addition to the electrical double layer capacitance of 36 F/g has been achieved by cyclic voltammetry at a scan rate of 50 mV/s and maintains at this level as the scan rate is increased up to 2000 mV/s. The maximum SC value can reach as high as ~365 F/g with chronopotentiometry in a mild neutral aqueous electrolyte (i.e., 0.10 M Na_2SO_4). This hybrid structure can be directly grown on thin conductive substrates including copper and tantalum foils, which can potentially be applied for large-scale industrial production.

Acknowledgment. We thank Lateef Syed and Qin Li for technical help with some experiments. J.L. thanks Kansas State University and Kansas Space Consortium for financial support. This work is also partially supported by the National Science Foundation under Award No. EPS-0903806 and matching support from the State of Kansas through Kansas Technology Enterprise Corporation.

Supporting Information Available: Histograms of the distribution of the outer diameter of carbon nanofibers and Manganese Oxide deposition sample, SEM and TEM images of an as-grown VACNF array directly coated with MnO_2, cyclic voltammograms of an as-grown VACNF arrays without subjecting to acid treatment and this sample after deposited with MnO_2 at various deposition time, X-ray diffraction spectrum of the manganese oxide after annealing in the air for 2 hrs at 200 °C showing α-MnO_2 crystal structure, the Bode plots of an acid-treated VACNF array, the Nyquist plot and fitting of electrochemical impedance spectra of samples without going through acid treatments, The Bode plots of as-grown VACNF array. This material is available free of charge via the Internet at http://pubs.acs.org.